Integrated Method for Rice Cultivation Monitoring Using Sentinel-2 Data and Leaf Area Index

***Abdelraouf M. Ali[1,2], Igor Savin[1], Anton Poddubsky[1] , Mohamed Abouelghar[2] and Nasser Saleh[2]**

[1] Agrarian-Technological Institute of the Peoples' Friendship University of Russia, ul. Miklukho-Maklaya 6, Moscow, 117198 Russia
[2] National Authority for Remote Sensing and Space Sciences, 23 Joseph Tito, El-Nozha Elgedidah, Cairo, Egypt.
* Correspondence:**orresponding Author**: massud-am@rudn.ru , Tel.+79015257326

Abstract Rice is an essential crop for national food security in Egypt. Increasing the population calls for regular increases in rice production. At the same time, cultivated rice crop areas should be decreased because of the gradual scarcity of irrigation water. This means more rice production should be gained from less rice area. This situation calls for the annual accurate system for rice monitoring and yield estimation. Therefore, it is necessary to apply a remotely sensed based system for rice cultivation assessment using satellite imagery parallel with field measurements of some biophysical parameters. Multi-temporal normalized difference vegetation index (NDVI) extracted from twelve sentinel-2 imagery cover the whole summer season with variance and maximum value assessed by ground control points (GCPs), were used to isolate uncultivated areas, then to isolate rice areas and other vegetation covers. object-based classification methods with kappa co-efficient 0.9261 and overall accuracy 94.92% was generated to discriminate rice crop area and other summer crops on the study area. Leaf area index (LAI) for the experiment the l site was calculated using the surface energy balance algorithm for Land (SEBAL) model and then tested versus measured (LAI). NDVI and LAI were used to generate empirical ran rice yield prediction model. Then, this model was used to produce rice to yield a map. The study was carried out in an experimental site in Kafr Elsheikh governorate with a total area of 5040 Hectare. Produced cultivated land use map showed 95% overall accuracy. High similarity was observed between measured and calculated (LAI) with high accuracy R2 = 0.94. of Rice, yield map showed expected yield more to than a month before harvest. The generated yield map was tested using a correlation coefficient between actual yield and estimated yield with high accuracy R2 = 0.9. This method is applicable to estimate acreage and productivity of rice in the north Nile delta in adequate time before harvest.

Keywords: Sentinal-2; NDVI; LAI; rice; yield

1. Introduction

Rice is the main staple food crop for a huge percentage of global population beside its role in global biogeochemical processes[1]. Rice agriculture may face major challenges in the coming decades due to increasing resource pressures, severe weather and climate change, population growth and economic development[2]. More than one billion people depend on rice to support diets and livelihoods. At the same time, the total accumulated area of rice has tapered off as available arable land is becoming scarce and competition for land uses evolve. This has resulted in intensified practices for additional crop cycles and production amplifying water utilization and management to enhance rice productivity.

In Egypt, rice is the dominant summer crop in Nile delta because of its low cultivation costs comparing with other summer field crops such as maize and cotton. It is the main food for about 50% of Egyptians, especially in the Nile Delta and northern Egypt [3]. The total rice area in Egypt is 510,648.6 hectare in 2015 produced 326,429 ton as reported by Ministry of Agriculture. Rice is cultivated mainly in northern Nile delta where the soil is characterized by high salinity. This situation forces large areas of northern Nile delta to cultivate rice in summer season as the huge amount of irrigation water that is consumed by rice enables periodical soil leaching and sustains

high level of soil productivity. Kafrelsheikh governorate that is in the northern of Nile delta is one of the top rice producers in Egypt with a total production of 13,749 ton produced from 104,577.5 hectare as reported in 2015. Starting from 2018[4], Egyptian government launched new legislation to reduce rice area to face the problem of expected scarcity of irrigation water. This may affect summer crop composition in large areas of Egyptian delta beside its effect on soil characteristics[5][6]. The current concern of agricultural research community is how to keep an adequate demand of rice production from less rice acreage and at the same time how to stop any degradation in soil characteristics as a result of decreasing rice areas. This relatively complex situation calls for an integrated system for rice crop monitoring. This is in which satellite imagery and ground measurements could be employed powerfully[7],[8][9][10].

One of the main components of rice crop monitoring is yield estimation. Basically, yield of the main cereal crops is a global issue related directly to food security and human life [11][12]. Crop yield estimation in an adequate time before harvest ensures more effective agricultural management policies. Ground-based method for crop yield estimation is commonly used worldwide; however, it is costly and time consuming. Therefore, applying an accurate, low costly effective and rapid, method for crop yield prediction at local and regional scales is one of the main objectives of remote sensing agricultural (RS) applications[7], [13]–[16].

The second component of rice crop monitoring system is crop biophysical parameters that are closely related to crop vigor and crop vegetative health and could be linked with crop productivity and crop spectroscopic parameters. Remote sensing is a powerful mean to study crop biophysical, biochemical and phonological parameters such as biomass [17], leaf area index (LAI)[18];[19][20]; [21], [22], and chlorophyll content [19] These parameters could be linked with remotely sensed data represented as vegetation indices (VIs). Many studies analyzed the relationship between one vegetation index and one or more of these parameters. Other studies analyzed the correlation between remotely sensed and measured parameters with crop yield. Linear correlation was found between normalized difference vegetation index (NDVI) and grain wheat yield [23], linear relationship addressed the correlation between wheat yield and band ratios (NIR/ Green) and (NIR/ Red) [11]. Absorbed photosynthetically active radiation (PAR) was used as an estimator for crop yield. In homogeneous large cultivated areas, Landsat and SPOT5 imagery with adequate spatial resolution of 30 m and 10 m were used for crop yield prediction [25],[7] [26]The objective of the current study is to propose a remote sensing-based system for rice crop monitoring using satellite data and ground measurements. The proposed models are applicable more than a month before harvest in any rice production area of Nile delta region of Egypt.

2. Material and Methods

2.1. Study area

The study was carried out in Kafr El-Sheikh governorate. Kafr El-Sheikh is located in the northern part of Nile Delta between Rosetta and Damietta Nile branches. The location of the governorate is between 31° 30` 7.59`` and 31° 9` 58.09`` North and between 30° 20` 36.83`` and 31° 17` 15.16`` East. It is bordered by Mediterranean Sea and Burulus Lake from the North, Behira governorate from the west, Dakhlia governorate from the east and Gharbia governorate from the south as shown in figure (1).

Preprints (www.preprints.org) | NOT PEER-REVIEWED | Posted: 21 December 2019 doi:10.20944/preprints201912.0282.v1

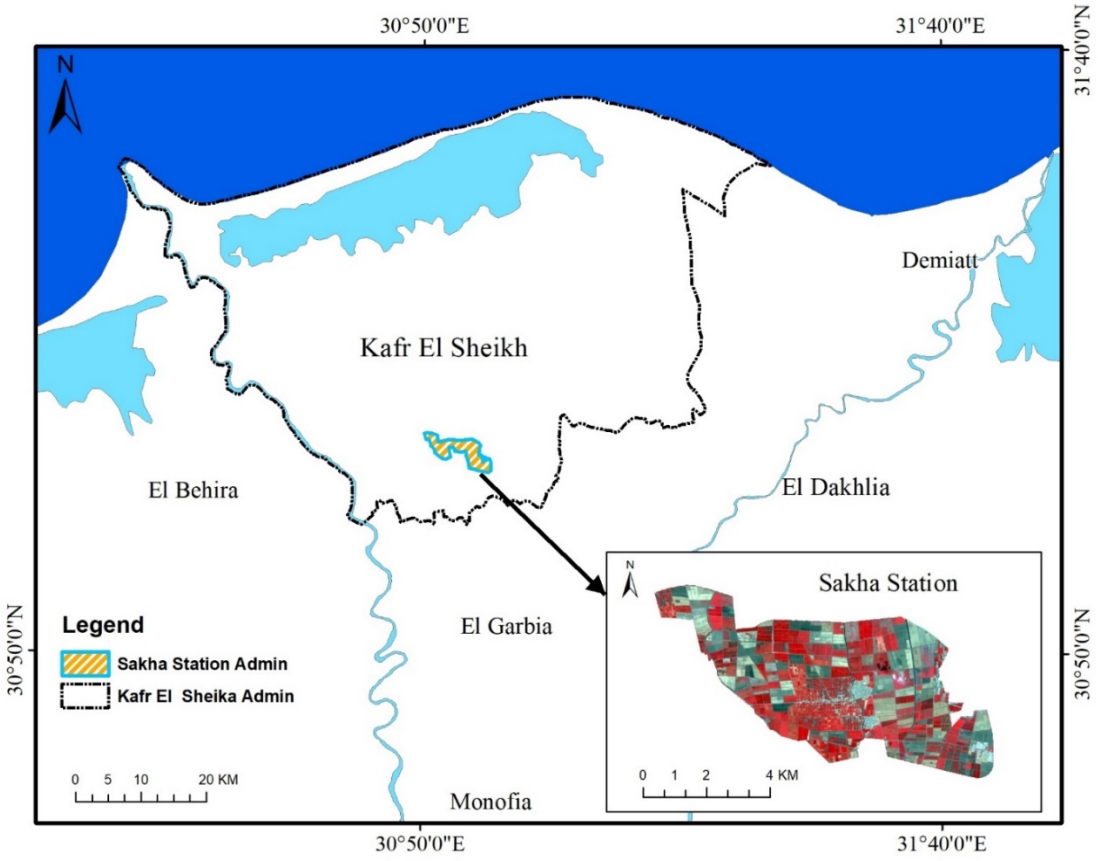

Figure 1. Study area (Sakha Agriculture research station - Kafr El-Sheikh governorate)

As a part of KafrElsheikh governorate, field measurements for rice biophysical parameters and generation of rice yield prediction models and generation of the modeling to retrieve biophysical parameters from vegetation indices were carried out in Sakha experimental station in KafrElsheikh governorate with a total area of 5040 hectare as shown in figure (2). Rice cultivation in Egypt is vital for national food security. At the same time, rice cultivation consumes huge amount of irrigation water when the national resources of irrigation water are relatively getting lower. The study area is located in Kafr ElSheikh governorate. Basically, nine governorates in Egypt cultivate rice every season with varying areas, however, Kafr ElSheikh governorate, where the study area of the current study is located, is a special case. This governorate is one of the top rice producers in Egypt. It occupies the second level over the country in terms of the area planted with the rice, while it the first in terms of productivity of the rice. It is coastal governorate and the soil of large areas is characterized as highly saline soil. Therefore, cultivating rice with large amount of water is necessary for salt leaching process, otherwise, large areas of the governorate will face severe degradation. In addition, cultivating rice increases underground water table which is a method to face coastal land erosion. This situation makes rice cultivation in Kafr ElSheikh governorate is one of the key factors in irrigation water management in Egypt.

The central government of Egypt launched legislations and regulations in order to decrease the total area of rice cultivation without any bad effect on soil characteristics. At the same time, intensive work is carried out to produce new rives varieties that are more tolerant to dry conditions. The final national objective is to keep the national amount of rice production with less consumption of irrigation water

 doi:10.20944/preprints201912.0282.v1

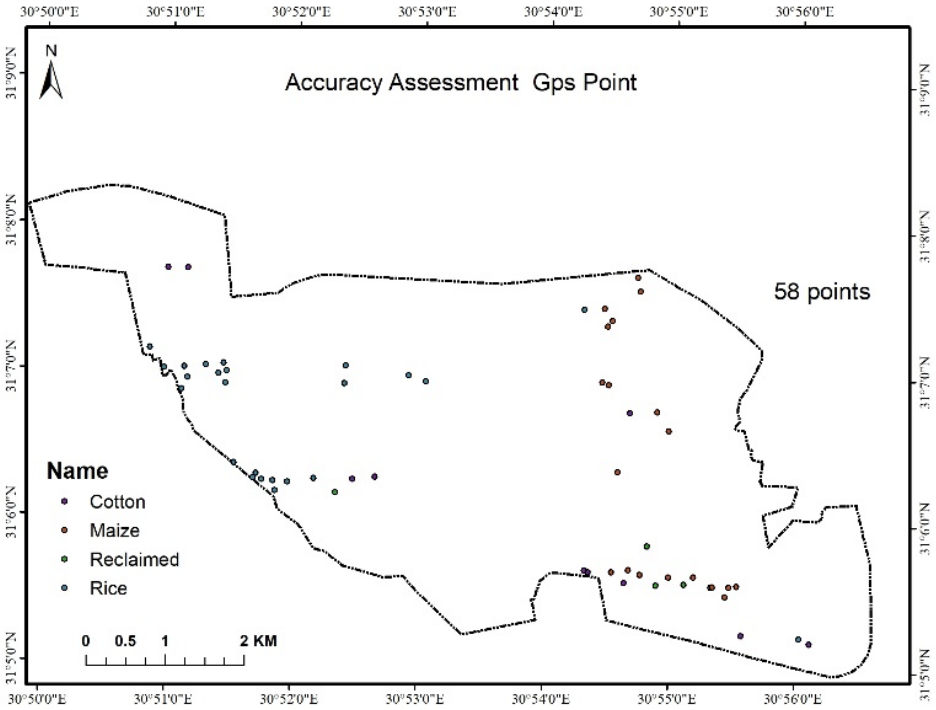

Figure 2: Distribution of ground control point for Accuracy assessment

2.2. Satellite data processing

Cultivated areas in Nile delta is are very dense, therefore, high spatial resolution satellite imagery (<= 20 meters) are necessary to accurately isolate any vegetation cover under investigation in Nile delta. Also, isolation of a specific crop type in the intensive cultivated areas in Nile delta requires multi-temporal satellite images [9] that cover the whole growing season of the crop. Therefore, nine sentinel-2 satellite images with ten meters spatial resolution that were expected to cover the whole rice growing stages of rice (preparation, emergency, tillering, flowering, repining and harvesting) during the season of 2018 were used in the current study figure (3).

Preprints (www.preprints.org) | NOT PEER-REVIEWED | Posted: 21 December 2019 doi:10.20944/preprints201912.0282.v1

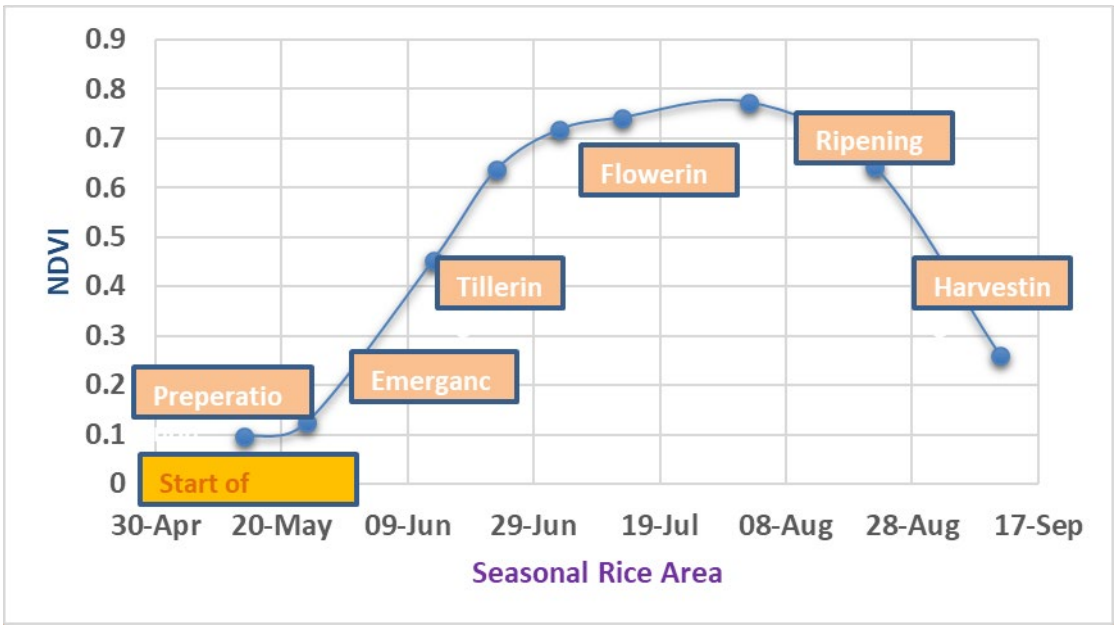

Figure 3. Phenology stages of a typical rice crop and their NDVI values

Sentinal-2 of multispectral product at 10-meter spatial resolution was downloaded from the ESA's Earth Observing System Data and Information System website. Image files were stored in the format SAFE with different spatial resolution as raster tiles/scenes. All preprocessing sages were performed including: re-projection, atmospheric correction, mosaic, sub setting, and layer stacking. The Atmospheric correction was carried out using (FLAASH - ENVI) module for senstinel-2 images. This module relies upon standard condition for unearthly brilliance at a sensor pixel, L. The condition of this module is as per the following in condition No (1) as indicated by [27]

$$L = \left(\frac{A\rho}{1-\rho e\, S}\right) + \left(\frac{B\rho e}{1-\rho es}\right) + La \qquad \text{Equation -1}$$

where:

ρ is the pixel surface reflectance

ρe is a normal surface reflectance for the pixel and an encompassing locale S is the spherical albedo of the atmosphere

La is the radiance back scattered by the atmosphere

A and B are coefficients that rely upon barometrical and geometric conditions yet not at first glance. Stacking is a process of combining multi layers into a single output file. A stacked image file was created through stacking 9 images using ENVI.3.1 (Version 2016).

2.3. Distribution of rice Area

Basically, methodology depends on major components, (i) determining the maximum and stander deviation of NDVI time series (ii) identifying the threshold value for NDVI to mask non cultivated areas (iii) multi resolution segmentation techniques and post classification methods to

Preprints (www.preprints.org) | NOT PEER-REVIEWED | Posted: 21 December 2019 doi:10.20944/preprints201912.0282.v1

identify rice signatures in temporal dimension (iv) classification calibration and validation; spatial distribution of rice area. These are described in the following subsections.

2.3.1. determining the maximum and stander deviation of NDVI time series

This resulted in a continuous sequence of NDVI temporal values for each pixel during the growing season. Normalized difference vegetation index (NDVI) Equation (2) was calculated for each individual image and assessment of (NDVI) values was carried out as shown in figure (4). The acquisition dates of the used satellite are: May 14, May 24, June 13, June 23, July 3, July 13, August 2, August 22 and September 1. Normalized difference vegetation index (NDVI) time series was calculated to be used

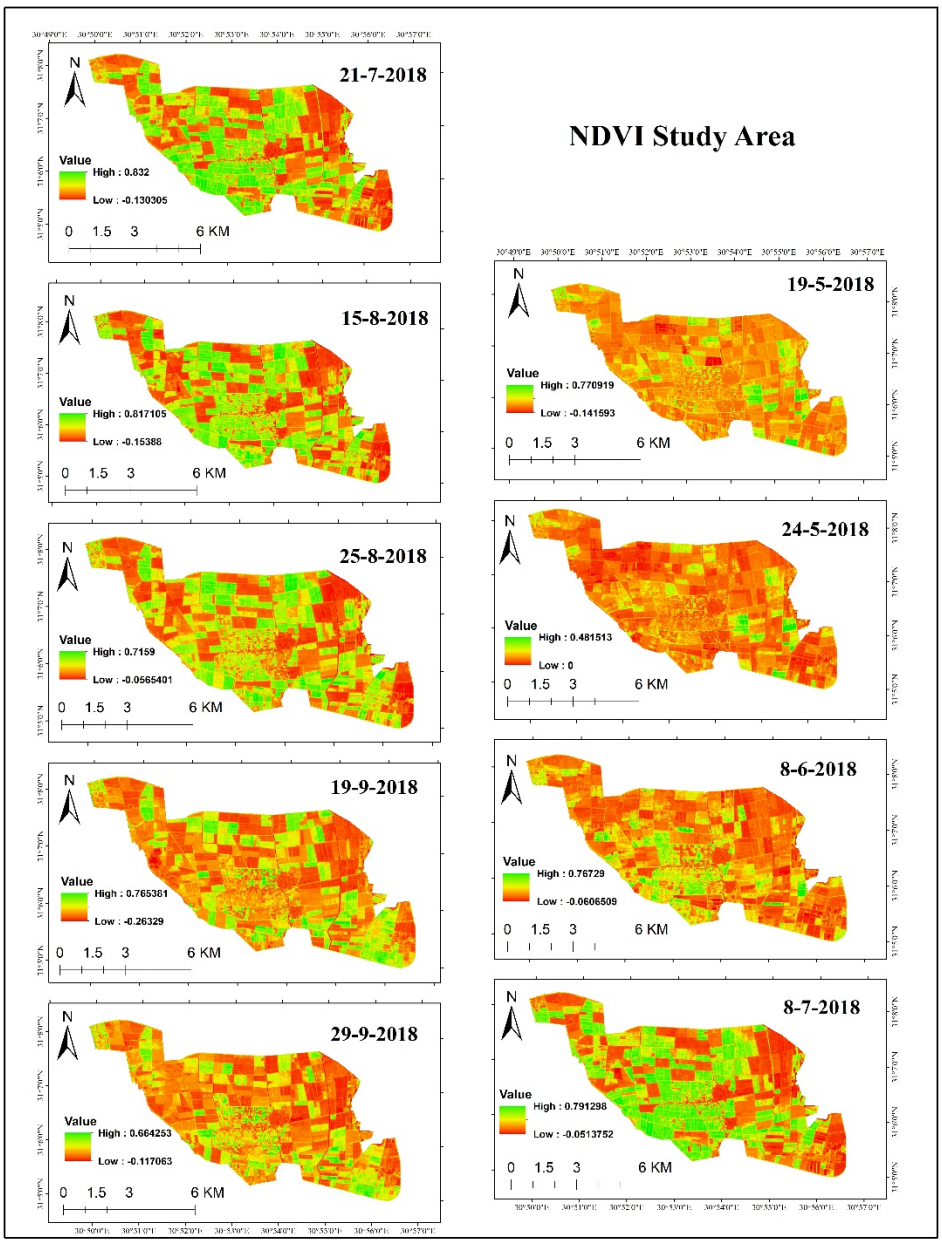

Figure (4) Data acquisition for sentinel-2 and NDVI images for the study area

for masking the non-Vegetated areas and isolate only vegetated areas. Normalized difference vegetation index (NDVI) was calculated for each single date. This index is calculated according to the following equation [2]:

 doi:10.20944/preprints201912.0282.v1

$$NDVI = \frac{\rho_{ir} - \rho_r}{\rho_{ir} + \rho_r}$$

(Equation 2)

Image segmentation was applied object-based segmentation with scale 10 the NDVI time-series through rice growth stage for the multitemporal dimension of rice season started from May to September 2018 in order to determine rice-specific signatures.

2.3.2. Identifying the threshold value for NDVI to mask non cultivated areas

For this technique, we considered having 5 classes by setting the convergence threshold of 0.85 as also reported by ([29] ; (Mosleh, 2015),(Ali et al. 2018) with the infinite number of iterations (the iteration would depend upon reaching to the desired convergence threshold). The explanation behind the adoption of this explicit agglomeration was its ability to: 1) assign each picture element to a category supported spectral and temporal similarities, 2) determine many classes based on inherent characteristics of the time-series and 3) discriminate a large area covered by different crop types.

The temporal signature was defined as a maximum NDVI values over the entire crop growth stages for each of the classes. Identification of this sig. nature including the creation of land use map as the first step in order to make sure the class of interest fell under agricultural land category

2.3.3. Multi resolution segmentation techniques and post classification methods to identify rice signatures in temporal dimension

high spatial resolution imagery of sentinel-2 were used to visually identify unique features related to rice plantation such as small field crops, irrigation structures (that include canals, irrigation channels, roads, etc.) ([32], (Ali et al., 2018). Assessment of NDVI trend as resulted from rice phenological information. The maximum and standard deviation for NDVI values of rice cultivation were used as additional input factors to maximize the accuracy of crop classification and isolation of rice cultivations.

The classification of the satellite imagery was used using object-based classification utilizing 4 bands of the Sentinal-2 images (B2,B3,B4 and b8) and the corresponding four bands. Before setting up the segmentation parameters, spectral bands of images were weighted proportional to the mean of pixel values at image band, which can be considered as a parameter of separability. After segmentation, a standard nearest-neighbor algorithm (with manual sample selection) was used to classify objects into 3-layers basic classes: Rice, Maize, cotton, and the other classes describe the bare soil (prepared land for agriculture) and Urban Area.

2.3.4. classification calibration and validation

the accuracy assessment and validation of classification was conducted using Kappa coefficient and over all accuracy. This analysis is a distinct multivariate procedure used to determine classification accuracy from an error matrix. It generates a Kappa coefficient that has a probable range from 0 to 1 equation 3 according to [33].

 doi:10.20944/preprints201912.0282.v1

$$K = \frac{N\sum_{i-1}^{r} x_{ii} - \sum_{i-1}^{r}(x_{i+}.x_{+i})}{N^2 - \sum_{i-1}^{r}(x_{i+}.x_{+i})}$$

(3)

There is one probable clarification of Kappa Coefficient: poor agreement = less than (0.20), fair agreement = (0.20) to (0.40), moderate agreement = (0.40) to (0.60), good agreement = (0.60) to (0.80), very good agreement = (0.80) to (1.00) figure (2) showed the distribution of ground control point.

2.4. Rice yield map

After we determine the spatial distribution map of rice as describe in the above, we performed the following three steps in evolving a rice yield map. Firstly, we started determine average NDVI-values (i.e., NDVI peak–greenness) depending upon our study on Sentinel- 2 to describes the spectral profile for rice crop and determine the rice phenology in the study area. The temporal profiles of NDVI of rice crop extracted from sentinel- 2 imagery were clearly unique in the study area to determine the peak greenness of rice during the peak greenness period (July 24th depending on NDVI time series). Secondly, we applied equation from SEBAL 2002 to calculate LAI depending on satellite imagery, thirdly, validated LAI index map using ground observation point and the pixel value of LAI using regression analysis between pixel value and measured LAI. Fourth mapping rice yield map depending on generated model by (Noureldin et al., 2013) finally, tested yield map using correlation coefficient between yield map and actual yield.

Rice yield map was estimated according to reported and tested empirical statistical model as describe on equation (4). The model was applied one month before harvesting. This model was generated and validated on the same study area.

$$\boldsymbol{Y = -3.110 + 1.684 * (LAI) + 12.458 * (NDVI)}$$

Equation 4

Where y: defined as the estimation yield, while (LAI): is the leaf area index. It was calculated from Equation 4. and NDVI: is the Normalize Difference vegetation index and its calculated from the peak greenness of rice crop growth stages

2.4.1. NDVI peak greenness

Assessment of NDVI profile throughout the season showed that in the beginning, associated with low biomass, the average NDVI values were significantly small. NDVI values increased gradually associated with the development of canopy to reach the peak value in August.

2.4.2. LAI measurements

Preprints (www.preprints.org) | NOT PEER-REVIEWED | Posted: 21 December 2019 doi:10.20944/preprints201912.0282.v1

LAI is the ratio of the total area of all leaves on a plant to the ground area represented by the plant. It is an indicator of biomass and canopy resistance. LAI was measured and computed using two approaches. One of them is using surface energy balance algorithm of land equation 5:

$$LAI = -\ln\left(\frac{0.069 - SAVI}{0.59}\right)/0.9$$

Equation 5

where; $SAVI_{ID}$ is the soil adjusted vegetation index calculated from Equation (6) using a value of 0.5 for L.

$$SAVI = \left(\frac{(Nir - Red)}{(NIR + REd + L)}\right) + (1 + L)$$

Equation 6

And the second methods of measuring LAI were also using ceptometer lP-80. This device measures the LAI of small plots, gapped, and non-uniform canopies simply and easily by restricting the view in terms of both azimuth (with view restricting caps) and zenith angles (by excluding one or more of the view rings). It is not possible to restrict either the azimuth or the zenith view angles using this device the methods was described by [35]

2.5. ArcGIs Model Builder for thrice spatial distribution.

Using the model-builder in Arc Map 10.4.0, a model was created for the respective test area. Once the LAI and NDVI variables of model were determined by the statistic models for Rice, the shape files with the source data were modified to reflect the attributes that contains the data of Rice area was used to extract raster value of different NDVI and LAI for Rice area from other crops area. Modeling process was applied for the peak-greenness growing stage (at August). Then, the model with the highest accuracy was applied to produce rice yield map. Based on the optimal generated statistical model was describe on figure (5)

2.6. Statically analysis for Validation maps.

The correlation coefficient between actual and predicted methods that was used to validate LAI and Yield maps. The statistical analysis was done using origin pro8 software

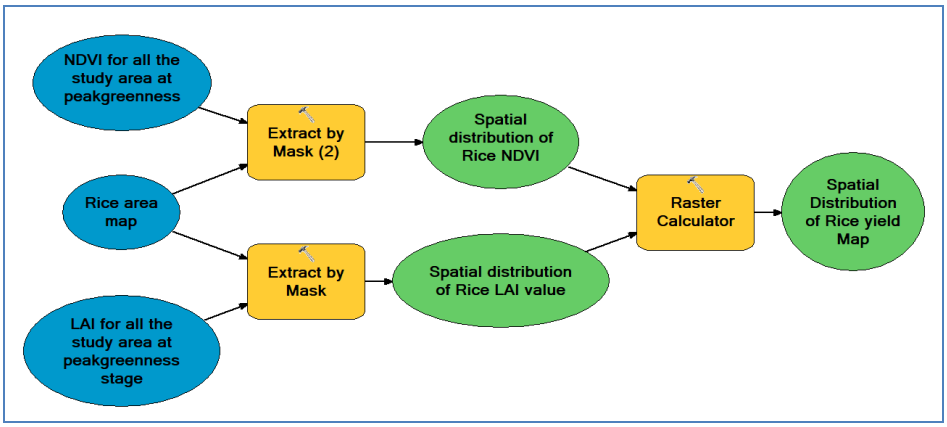

Figure 5 Model builder using Arcmap 10.4

Preprints (www.preprints.org) | NOT PEER-REVIEWED | Posted: 21 December 2019 doi:10.20944/preprints201912.0282.v1

3. Result:

3.1. Spatial distribution of rice area

The spatial distribution of rice area for the study area through year 2018 was estimation using object-based classification and mapped the spatial extent of cultivated crops on the study area in Figure 8(a and b). Depending on applying the thresholds determined we started to delineate the agriculture area (vegetated area) and non-agriculture Area as showed on figure (8c). object-based classification method for determination of crop areas under the study area to discriminate spatial distribution of rice area, we applied them over NDVI time series during rice season. It is achieved high accuracy method to discriminate between different types of crops and distinguishes the spatial distribution of rice crop in the study area. depending on NDVI threshold cross matched the phenology responses of cotton, rice, and Maize to filter out the rice area precisely. It revealed strong high accuracy with over all accuracy 94.92% and kappa co-officiant 0.921 as described on table (1) and figure 7. Our results were also similar to other studies: [36] used Landsat-derived vegetation indices, such as NDVI, EVI, and Mosleh et al., 2016 used MODIS vegetation indices time series, and (Ali et al. 2018) used sentinel- 2 to estimate winter crops in Egypt. We found that the study site remained under rice cultivation extensively was 1699.8 (Ha) and the weight of cotton around vegetation was 129. from the total area while maize represented around 327.35 (Ha). The spatial distribution of the area under rice cultivation is mapped in figure Figure 7.

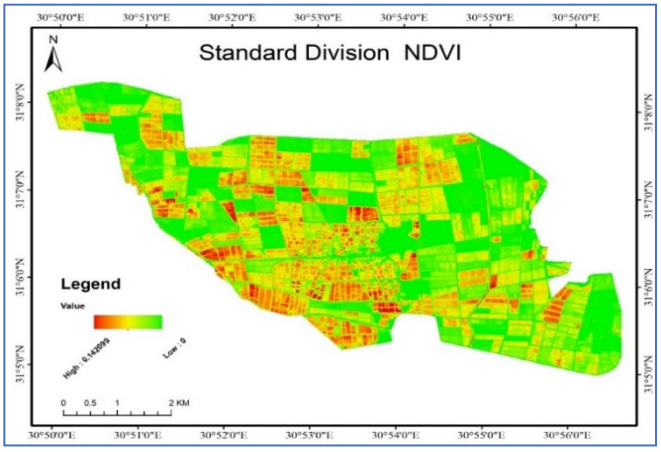

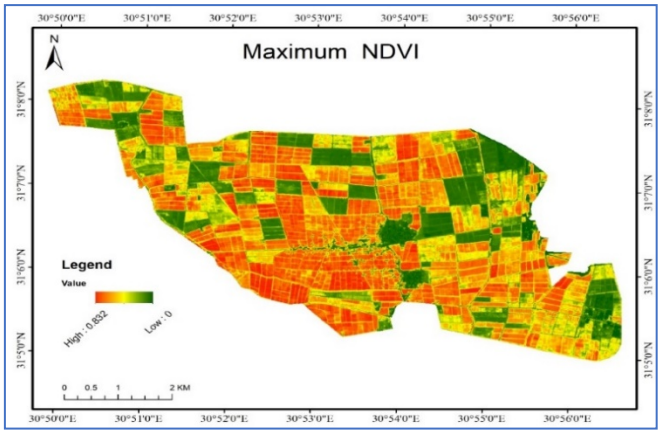

Preprints (www.preprints.org) | NOT PEER-REVIEWED | Posted: 21 December 2019 doi:10.20944/preprints201912.0282.v1

(6a)

(6b)

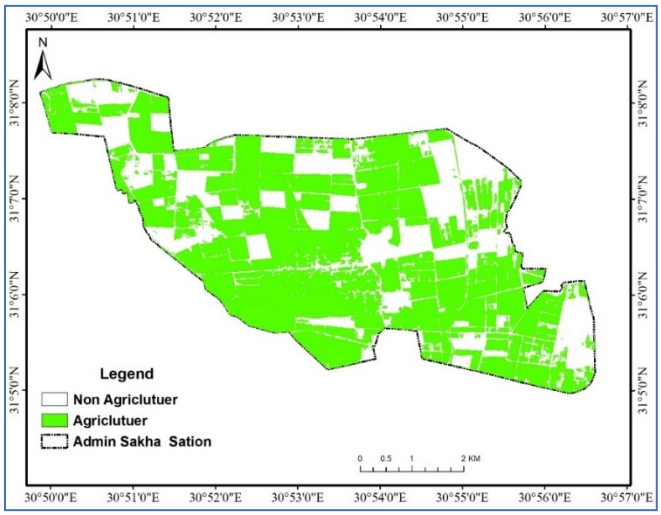

(6C)

Figure (6): (6a) Standard division of NDVI values sakha area (6b) maximum NDVI values for sakha area derived from multitemporal Sensinal -2 derived from multitemporal Sensinal -2 and (6C) Agriculture and non-Agriculture area derived by using maximum and standard division NDVI

Table (1) Kappa co-efficient and over all accuracy for crop area maps o the study area

 doi:10.20944/preprints201912.0282.v1

	NDVI time series
Kappa Coefficient	**0.9261**
Overall Accuracy	**94.92%**

318

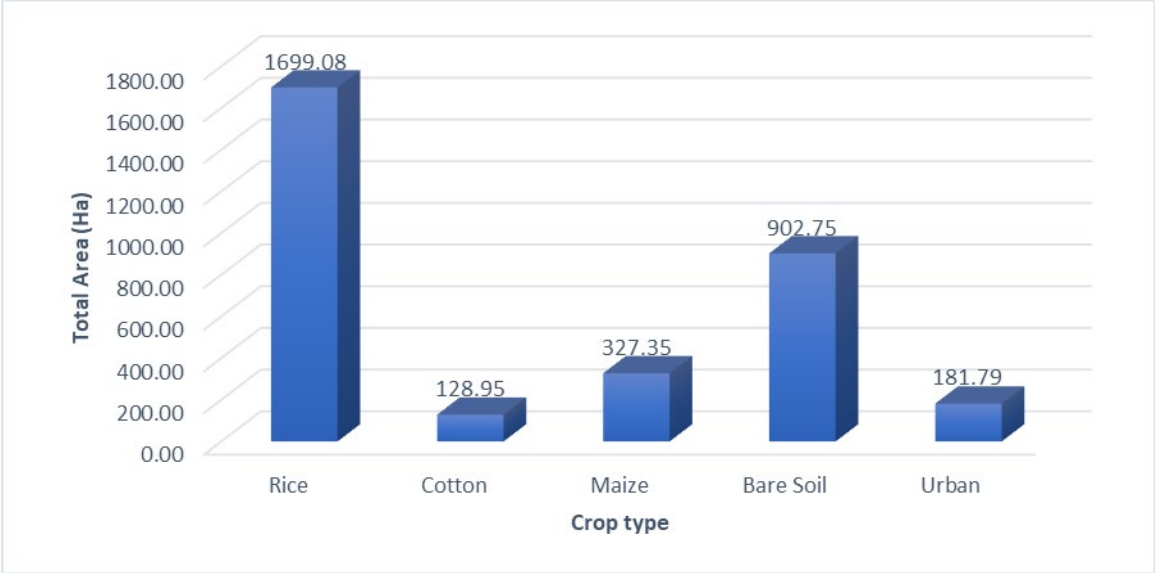

319

320 **Figure (7)** Total area for the discriminated crops on the study Area

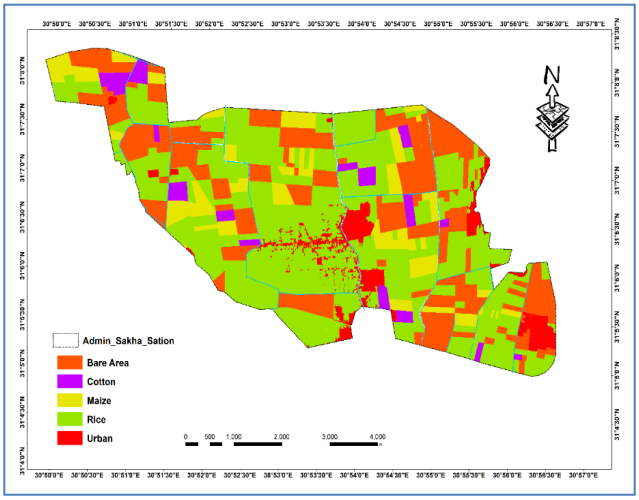

321

322

Preprints (www.preprints.org) | NOT PEER-REVIEWED | Posted: 21 December 2019 doi:10.20944/preprints201912.0282.v1

Figure (8-a) in the left derived rice cultivation area (indicated using green shades) mapping during 2018 and. **Figure (8-b)** on the right the boundary of rice cultivated on the study area

3.2. SEBAL LAI estimation as a factor to estimate rice yield.

Two variables were calculated to estimate rice yield map according to (noureldein et al., 2013) . one of the two variables is LAI. Its calculated as describe of section (5.2) to produce LAI map for rice cultivation. According LAI Map produced to show the gradual increasing then decreasing of LAI according to the growing circle of summer crops through (8 August) on the study area as shown on figures (9). LAI maps were validated by using actual LAI that measured by comptometer lp-80 using through peak greenness. The correlation between actual LAI and predicted LAI on the peek greenness period of Rice crop growth stage was used to calibrate LAI Map., as showed on Figure (10) The accuracy of the result achieved very high accuracy with R2 0.939 as, the second variable of NDVI was calculated from Sentinel 2 with the same time of measuring LAI.

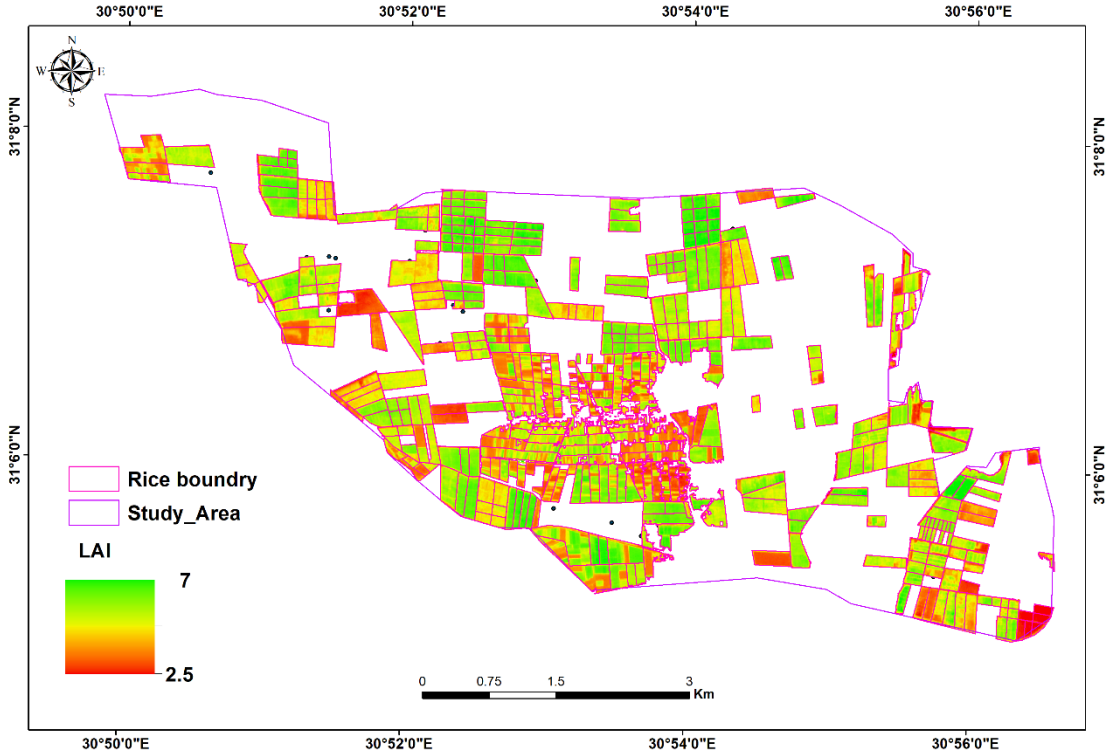

Figure (9). Estimated LAI depending on SEIBAL model Through August 2018 for different crops including maize and rice….

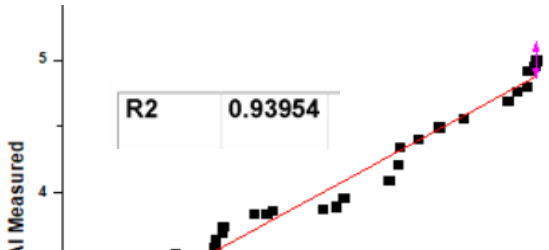

 doi:10.20944/preprints201912.0282.v1

Figure (10) (LAI Map validation) the correlation coefficient between LAI values at the peak greenness period (August) and ground-based rice LAI Measured by Ceptometer LP-80. It demonstrated strong relationships (i.e., *r*2.0.93).

3.4. Spatial distribution of Rice crop.

The model builder output consists of grid cells with values for estimated yield prediction in ton/Ha. The grid cell size used in the calculation was 10 square meters. The grid cell output was converted into polygon format so that calculations could be made to multiply each yield prediction rate by its area to determine the yield prediction for each Pixel. Figure (10) shows the yield prediction map for wheat crop in test area. This map shows that the vegetative Crop growth stage was the best models for different NDVI models for peak greenness stage which has the best correlation coefficient for yield prediction models.

predicted results were validated using 54 validation sites in the Sakha station area of kafr Elsheikh governorate Figures 2. The results presented in figure 11 indicate that the estimated rice yield map was spatially variable among the sampling sites, the correlation coefficient observed in Figure 12 was implemented in forecasting rice yield during 2018; It showed that strong correlation coefficient (i.e., r2, =0.95) between ground-based (Actual yield) and forecasted yields at Sakha station. Rice yield map was carried out using the analysis of NDVI multi-temporal. This approach has been used in many studies using NDVI from NOAA/AVHRR and MODIS images [37] et al., 2003, [30]

Preprints (www.preprints.org) | NOT PEER-REVIEWED | Posted: 21 December 2019 doi:10.20944/preprints201912.0282.v1

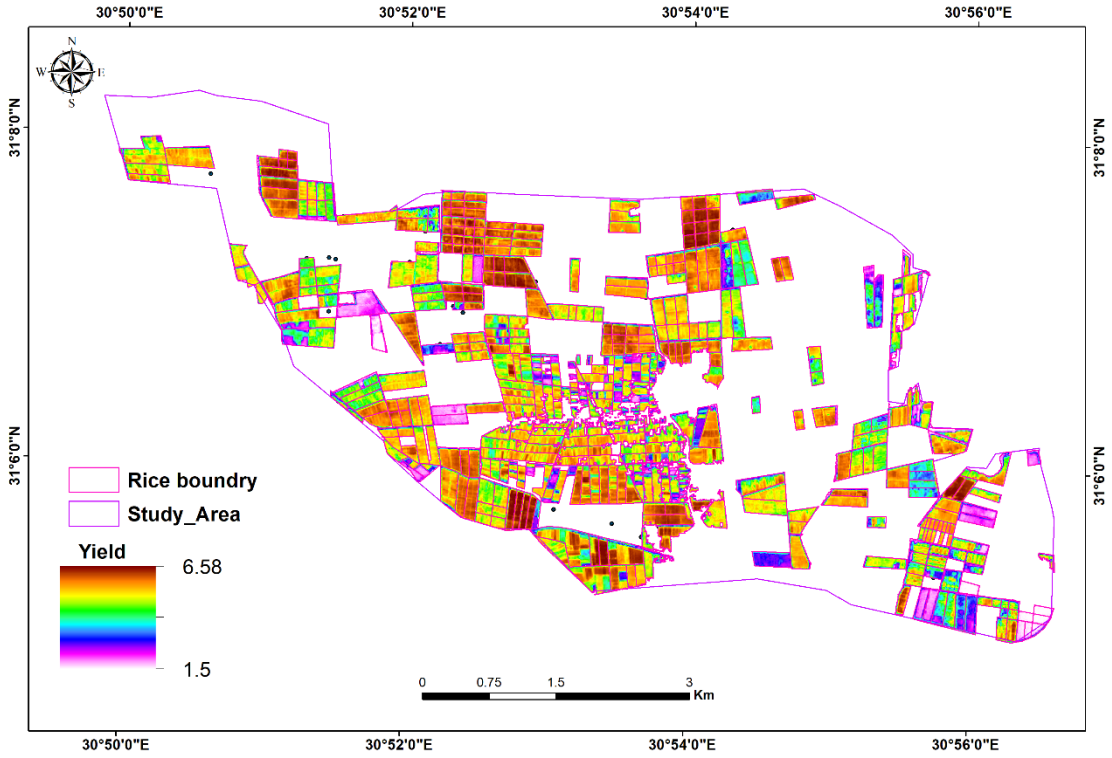

371

372 **Figure (11)** Spatial distribution of rice yield map for Sakha station

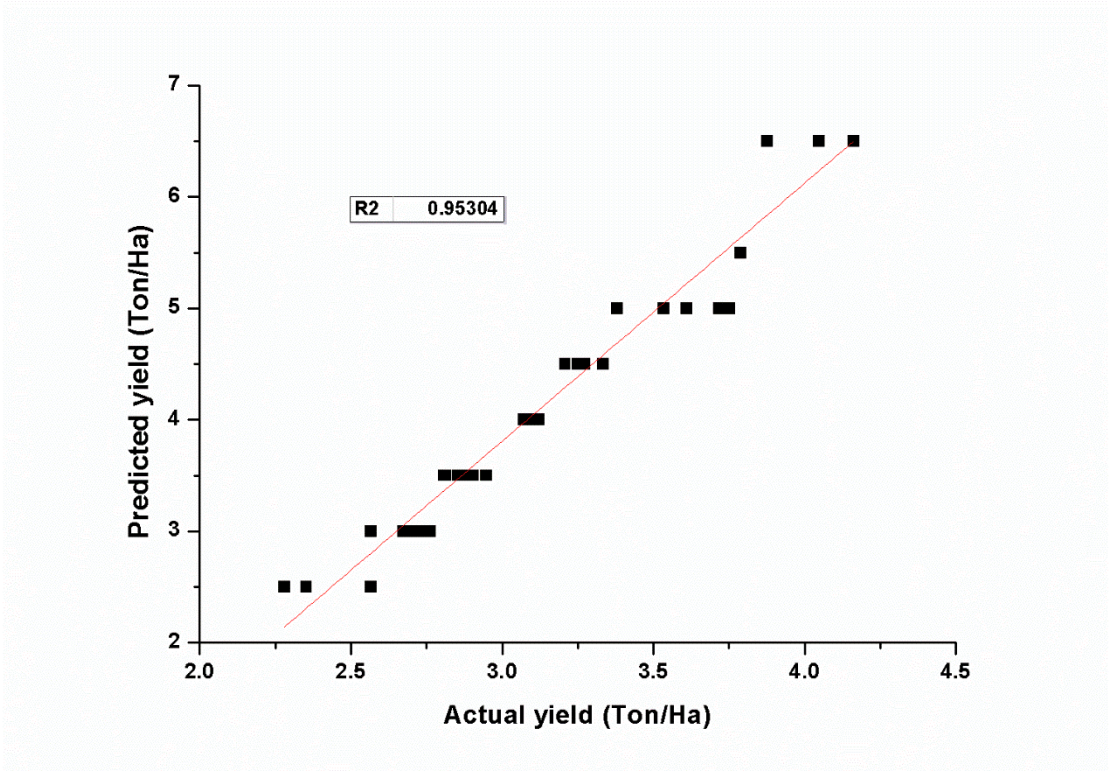

373

374 Figure (12) shows the relationship between yield values that we can predict it at the peak
375 greenness period (August) and ground-based Measured (actual yield. It demonstrated
376 strong relationships (i.e., *r*2.0.95).

377

4. Conclusion:

in this study new technology was implemented a new methodology to estimate the spatial distribution of rice area and rice yield pattern. This methodology was applied and tested under Sakha station. Multi temporal NDVI derived from sinteinal-2 satellite imagery was conducted to study the spatial distribution of rice area. It's used also to determine the peak greenness of vegetative growth stage to estimate and mapping rice area. The threshold values of maximum and standard deviation of NDVI was calculated to discriminate agriculture and non-Agriculture area. The object-based segmentation techniques using e-cognation developer software with spatial scale 10 m was used to determine the boundary and shape of different crops. five classes were determined on the study area. The kappa coefficient and overall accuracy were 0.9261 and 94.9 respectively. The spatial distribution of rice yield map was calculated according two variables as described on section (3.4), LAI was calculated according SEBAL model. The produced maps were validated using correlation co-efficient between measured and predicted LAI With high accuracy $R^2 = 0.93$. the ARC GIs model builder was used to determine the spatial distribution of yield map for each pixel. fifty-four ground yield were used to validate yield map with high accuracy 0.9. Finally, we are recommended to use this methodology with high accuracy to estimate rice area and yield on delta Egypt because of fragmentation of agriculture field crops.

References

1. C. Change and F. Security, *THE STATE OF FOOD AND AGRICULTURE*. 2016.
2. *The future of food and agriculture Trends and challenges*. .
3. W. Ghidan and M. Yacout, "Genetic Variability among Egyptian Rice Genotypes (Oryza sativa L .) for Their Tolerance to Cadmium Genetic Variability among Egyptian Rice Genotypes (Oryza sativa L .) for Their Tolerance to Cadmium," no. January, 2016.
4. H. Sayed, A. Abdelaal, and D. Thilmany, "Grains Production Prospects and Long Run Food Security in Egypt," pp. 1–17, 2019.
5. M. B. K. Le, "Proposal Application Form."
6. *Water Saving In Irrigated Agriculture in Egypt*. .
7. I. Ahmad, A. Ghafoor, M. I. Bhatti, I. H. Akhtar, and M. Ibrahim, "Satellite Remote Sensing and GIS based Crops Forecasting & Estimation System in Pakistan."
8. M. Boschetti *et al.*, "PhenoRice: A method for automatic extraction of spatio-temporal information on rice crops using satellite data time series," *Remote Sens. Environ.*, 2017.
9. A. M. Ali, M. A. Aboelghar, M. A. El-shirbeny, and N. H. Salem, "Comparative analysis of some winter crops area estimation using landsat-8 and sentinal-2 satellite imagery," *Futur. Food J. Food, Agric. Soc.*, vol. 6, no. 2, 2018.
10. Y. A. Detection, "Using Low Resolution Satellite Imagery for Yield Prediction," pp. 1704–1733, 2013.
11. G. Zhang *et al.*, "Mapping paddy rice planting areas through time series analysis of MODIS land surface temperature and vegetation index data," *ISPRS J. Photogramm. Remote Sens.*, 2015.
12. T. Liu, X. Liu, M. Liu, and L. Wu, "Evaluating heavy metal stress levels in rice based on remote sensing phenology," *Sensors (Switzerland)*, vol. 18, no. 3, 2018.
13. T. Paper, "REMOTE SENSING AND ITS APPLICATION IN AGRICULTURAL PEST," no. June, pp. 43–61, 2015.
14. M. K. Mosleh, Q. K. Hassan, and E. H. Chowdhury, "Application of remote sensors in mapping rice area and forecasting its production: A review," *Sensors (Switzerland)*, vol. 15, no. 1, pp. 769–791, 2015.
15. N. A. Noureldin, M. A. Aboelghar, H. S. Saudy, and A. M. Ali, "Rice yield forecasting models using satellite imagery in Egypt," *Egypt. J. Remote Sens. Sp. Sci.*, vol. 16, no. 1, pp. 125–131, 2013.
16. J. Dong *et al.*, "Mapping paddy rice planting area in northeastern Asia with Landsat 8 images, phenology-based algorithm and Google Earth Engine," *Remote Sens. Environ.*, 2016.
17. A. Gitelson, "Remote Sensing Estimation of Crop Biophysical Characteristics at Various Scales," no. May, 2016.
18. M. Aboelghar *et al.*, "Using SPOT data and leaf area index for rice yield estimation in Egyptian Nile delta," *Egypt. J. Remote Sens. Sp. Sci.*, vol. 14, no. 2, pp. 81–89, 2011.

19. D. Haboudane, J. R. Miller, N. Tremblay, P. J. Zarco-tejada, and L. Dextraze, "Integrated narrow-band vegetation indices for prediction of crop chlorophyll content for application to precision agriculture," vol. 81, pp. 416–426, 2002.
20. A. Verger, N. Vigneau, C. Chéron, J. Gilliot, A. Comar, and F. Baret, "Remote Sensing of Environment Green area index from an unmanned aerial system over wheat and rapeseed crops," *Remote Sens. Environ.*, vol. 152, pp. 654–664, 2014.
21. S. Liang, M. E. Schaepman, and M. Kneubuehler, "Remote Sensing Signatures : measurements , modeling and applications CHAPTER 10 Remote sensing signatures : Measurements , modelling and applications," no. May 2014, 2008.
22. A. M. Ali and M. Aboelghar, "Comparative Analysis of Different Methods of Leaf Area Index Estimation of Strawberry under Egyptian Condition," vol. 8, no. 1, pp. 2963–2970, 2019.
23. C. J. Tucker and B. N. Holben, "Remote Sensing of Total Dry-Matter Accumulation in Winter Wheat," vol. 189, 1981.
24. S. Pradhan, K. Bandyopadhyay, R. N. Sahoo, and V. K. Sehgal, "Predicting Wheat Grain and Biomass Yield Using Canopy Reflectance of Booting Stage," no. May, 2014.
25. M. M. Awad, "Toward Precision in Crop Yield Estimation Using Remote Sensing and Optimization Techniques," 2019.
26. P. Yang, G. X. Tan, Y. Zha, R. Shibasaki, R. Planning, and V. Indices, "INTEGRATING REMOTELY SENSED DATA WITH AN ECOSYSTEM MODEL TO ESTIMATE CROP YIELD IN NORTH CHINA," no. 1988, 2003.
27. R. Frouins *et al.*, "Passive remote sensing of tropospheric correction for the aerosol effect aerosol and atmospheric," vol. 102, no. 97, pp. 815–830, 1997.
28. E. Version, "ENVI Tutorials," 2000.
29. M. Kalácska, "Calibration and assessment of seasonal changes in leaf area index of a tropical dry forest in different stages of succession," no. August, pp. 733–744, 2018.
30. M. K. K. Mosleh, "Use of GIS and Remote Sensing in Mapping Rice Areas and Forecasting Its Production at Large Geographical Extent," p. 169, 2015.
31. A. M. Ali, S. Sciences, M. A. El-shirbeny, S. Sciences, N. H. S. Saleh, and S. Sciences, "Comparative analysis of some winter crops area estimation using landsat-8 and sentinal-2 satellite imagery," no. July, 2018.
32. J. Dong *et al.*, "Tracking the dynamics of paddy rice planting area in 1986-2010 through time series Landsat images and phenology-based algorithms," *Remote Sens. Environ.*, 2015.
33. Y. J. Kaufman, A. E. Wald, L. A. Remer, B. Gao, R. Li, and L. Flynn, "The MODIS 2 . 1- m Channel — Correlation with Visible Reflectance for Use in Remote Sensing of Aerosol," vol. 35, no. 5, pp. 1286–1298, 1997.
34. N. A. Noureldin, M. A. Aboelghar, H. S. Saudy, and A. M. Ali, "Rice yield forecasting models using satellite imagery in Egypt," *Egypt. J. Remote Sens. Sp. Sci.*, vol. 16, no. 1, 2013.
35. F. Ecology, E. Unit, P. Team, and F.- Champenoux, "Ground-based measurements of leaf area index : a review of methods , instruments and current controversies," vol. 54, no. 392, pp. 2403–2417, 2003.
36. J. Huang, "Rice yield estimation using remote sensing and simulation model," no. 2012, 2015.
37. Y. Qian *et al.*, "Crop Growth Condition Assessment at County Scale Based on Heat-Aligned Growth Stages."